



A duplex quantitative real-time PCR assay for the detection and quantification of *Xanthomonas phaseoli* pv. *dieffenbachiae* from diseased and latently infected anthurium tissue

Emmanuel Jouen^a, Frédéric Chiroleu^a, Véronique Maillot-Lebon^a, Aude Chabirand^b, Sabine Merion^c, Claudine Boyer^a, Olivier Pruvost^{a,1}, Isabelle Robène^{a,*,1}

^a UMR PVBMT, CIRAD, F-97410 St Pierre, Reunion island, France,

^b Unit for Tropical Pests and Diseases, Plant Health Laboratory (LSV), French Agency for Food, Environmental and Occupational Health & Safety (ANSES), St Pierre, Reunion Island, France

^c FDGDON, Clinique du Végétal[®], F-97410 St Pierre, Reunion Island, France

ARTICLE INFO

Keywords:

Real-time quantitative PCR
Xanthomonas phaseoli pv. *dieffenbachiae*
Diagnostics
Anthurium
Latent infections

ABSTRACT

Anthurium bacterial blight caused by *Xanthomonas phaseoli* pv. *dieffenbachiae* (formerly *Xanthomonas axonopodis* pv. *dieffenbachiae*) is the major phytosanitary threat in many anthurium growing areas worldwide. Reliable and sensitive diagnostic tools are required for surveillance and certification programs. A duplex real-time quantitative PCR assay was developed for the detection and quantification of *X. phaseoli* pv. *dieffenbachiae* from anthurium tissue. This PCR assay targeted a *X. phaseoli* pv. *dieffenbachiae*-specific gene encoding an ABC transporter and an internal control encoding for chalcone synthase in *Anthurium andreaeanum*. A cycle threshold (Ct), using a receiver-operating characteristic approach (ROC), was implemented to ensure that the declaration of a positive sample was reliable. The duplex real-time assay displayed very high performance with regards to analytical specificity (100% inclusivity, 98.9% exclusivity), analytical sensitivity (LOD_{95%} = 894 bacteria/ml corresponding to 18 bacteria per reaction) and repeatability. We demonstrated the pertinence of this real-time quantitative PCR assay for detecting *X. phaseoli* pv. *dieffenbachiae* from diseased leaf tissue (collected from outbreaks on anthurium) and from asymptomatic, latently infected anthurium plants. This assay could be useful for surveillance, as well as for indexing propagative plant material for the presence of *X. phaseoli* pv. *dieffenbachiae*.

1. Introduction

Misidentifying minor/opportunistic pathogens as quarantine pathogens can have a major negative economic impact, as shown by the citrus bacterial spot disease outbreak in the USA, in the 1980s (Schouties et al., 1987). One example from the genus *Xanthomonas*, where pathological convergence (i.e. a phenomenon where genetically distant strains of a pathogen cause same/similar symptoms on a given plant species) has been reported on some plant species in the Araceae family, is *X. axonopodis* pv. *dieffenbachiae*. It has long been recognized as a polyphyletic pathovar with strains that differ, both phenotypically, genetically and in terms of host range. Yet, they produce morphologically similar symptoms, especially in the early stages of outbreaks (Berthier et al., 1993; Chase et al., 1992; Lipp et al., 1992). Recently,

the strains of *X. axonopodis* pv. *dieffenbachiae* were reclassified into three species using a polyphasic taxonomic approach, based on Multi-locus Sequence Analysis (MLSA), DNA:DNA hybridization, Average Nucleotide Identity (ANI) values derived from complete genome data and phenotypic analyses (Constantin et al., 2016). Strains isolated from anthurium, as well as from some other aroid genera, responsible for anthurium bacterial blight (ABB) were included in the *X. phaseoli* species as *X. phaseoli* pv. *dieffenbachiae*. Strains that cause the bacterial leaf blight of syngonium (LBS) are aggressive on this plant species, but are not pathogenic to anthurium and weakly pathogenic to other aroid genera (Chase et al., 1992; Constantin et al., 2017). These strains were also classified in *X. phaseoli* as *X. phaseoli* pv. *syngonii* (Constantin et al., 2016). Strains originating from other aroid genera were reclassified in the *X. euvesicatoria* (referred to as Philodendron strains) and *X. citri* (as

* Corresponding author.

E-mail address: isabelle.robene@cirad.fr (I. Robène).

¹ O. Pruvost and I. Robène contributed equally to this work.

X. citri pv. *aracearum*) species (Constantin et al., 2016). They are primarily pathogenic to their host of origin and slightly pathogenic to anthurium or not at all (Chase et al., 1992; Lipp et al., 1992; Robene-Soustrade et al., 2006). Lastly, *X. arboricola* pv. *zantedeschiae* was reported as a pathogen of the aroid species *Zantedeschia aethiopica* (Joubert and Truter, 1972; Parkinson et al., 2009), although it was not investigated by Constantin et al.

Anthurium (*Anthurium andreaeanum* Linden ex André) is the second most important tropical flower crop cultivated in the world. This very popular ornamental crop is threatened by the pathogen *Xanthomonas phaseoli* pv. *dieffenbachiae*, the causal agent of ABB, which is subject to various regulations in different parts of the world (<https://gd.eppo.int/taxon/XANTDF/categorization>). On anthurium, leaf symptoms start as water-soaked spots, frequently visible near the margins (i.e. the pathogen typically infects anthurium through hydathodes), which become surrounded by yellowish areas and gradually turn brown. The pathogen moves into vascular tissues, eventually causing plant death on susceptible anthurium cultivars. Blight symptoms can also be observed on spathes (Alvarez et al., 2006). There are no reports worldwide of outbreaks on anthurium caused by *X. citri* pv. *aracearum*, *X. euvesicatoria* “Philodendron” or *X. phaseoli* pv. *syngonii*. To our knowledge, no strain of these taxa (sampled from naturally infected anthurium) are available in culture collections. However, some aroid species (e.g. in the genera *Aglaonema*, *Alocasia*, *Caladium*, *Philodendron*, *Syngonium* or *Xanthosoma*) (Chase et al., 1992; Constantin et al., 2017; Dickey and Zumoff, 1987) can host both *Xanthomonas phaseoli* pv. *dieffenbachiae* and at least one other *Xanthomonas* taxon. ABB was first described in 1952 in Brazil (Robbs, 1955). It has been thereafter reported from numerous countries, and outbreaks or incursions of the pathogen were repeatedly recorded in association with anthurium in Europe and other Mediterranean countries (Fig. S1).

The control of ABB depends mainly on the success of sanitation and prophylactic measures. Thus, it requires early and accurate detection of latently infected plant material. Improvement in diagnostic protocols for *X. phaseoli* pv. *dieffenbachiae* have recently been achieved. To isolate the bacterium, a new semi-selective medium (NCTM4) has been developed, which promotes more efficient bacterial growth than the media CT and ET, commonly used in detection protocols (Laurent et al., 2009). Specific molecular tools are available for this pathogen: a nested-PCR assay (N-PCR) (Robene-Soustrade et al., 2006) and a loop-mediated isothermal amplification assay (Lamp) (Niu et al., 2015). The N-PCR is specific and sensitive (detection threshold = 10^3 CFU/ml) and has recently been validated through comparative and collaborative studies (Chabirand et al., 2014). It has since been included in a revised version of the Eppo detection protocol (Anonymous, 2009). Nevertheless, the major drawback of N-PCR assays is the high risk of cross-contamination because sample tubes need to be opened between the two rounds of amplification. It is interesting to note that the Lamp assay is adapted to the on-site detection of the pathogen. However, its analytical sensitivity is lower than the N-PCR (10^4 CFU/ml) and, consequently, it is probably less efficient in detecting latent infections.

Real-time quantitative PCR assays tend to displace conventional PCR in detection protocols. The technique can be used to quantify the pathogen in samples and is also highly sensitive, which means that a large number of samples can be managed. In addition, the risks of cross-contamination are decreased drastically because all steps are performed in a contained system. Recent examples include *X. arboricola* pv. *pruni* (Palacio-Bielsa et al., 2011), *X. albilineans* (Garces et al., 2014) and *X. euvesicatoria* pv. *allii* (Robene et al., 2015).

The quality of nucleic acid in biological samples is highly dependent upon the conditions of sample acquisition and storage and subsequently the extraction method used. The addition of an internal control in the qPCR assay that will be handled, stored, co-extracted and co-amplified with the target DNA in the chain of processing is a good way to check for incomplete recovery of DNA or the presence of PCR inhibitors. This internal control can be a “competitive” internal control involving a

pseudo-target with primer binding regions identical to that of the target region (Muska et al., 2007), or also a non-competitive internal control sequence that can be endogenous RNA or DNA sequences present in the sample (Ioos et al., 2009; Li et al., 2006).

Here we developed a real-time duplex quantitative PCR assay for the detection and the quantification of *X. phaseoli* pv. *dieffenbachiae* from anthurium tissue, which included an internal control targeting an endogenous anthurium gene. Interestingly, this detection assay excludes other xanthomonads pathogenic to some aroid genera, including the closely-related strains of *X. phaseoli* pv. *syngonii*.

2. Materials and methods

2.1. Bacterial strains, culture conditions and characterization

The bacterial strains used in this study included 81 aroid xanthomonads and 61 other bacterial strains (Tables S1 and S2). Strains were stored at -80°C in Microbank™ cryovials for long-term storage and routinely grown on YPGA medium (7 g/l yeast extract, 7 g/l peptone, 7 g/l glucose, 18 g/l agar, 20 mg/l propiconazole; pH 7.2) at 28°C .

Aroid *Xanthomonas* strains were authenticated (Tables S1 and S2) as a preliminary step of our study by multilocus sequence analysis (MLSA), using four housekeeping gene portions (*atpD*, *dnaK*, *efp* and *gyrB*) as previously reported (Bui Thi Ngoc et al., 2010; Hamza et al., 2012). The sequences were deposited in the GenBank database.² Additional sequence data were obtained from Bui Thi Ngoc et al. (2010) or Hamza et al. (2012).

A maximum likelihood tree, computed from the concatenated dataset with PhyML 3.0.1 (Guindon and Gascuel, 2003), with a bootstrap analysis (1000 resamplings), considering the GTR + Γ + I DNA substitution model, and rooted with *X. oryzae* pv. *oryzae*, allowed a clear-cut delineation of each group of strains (Fig. S2). *X. phaseoli* pv. *dieffenbachiae* (four distinct Sequence Types³ (ST)) differed from *X. phaseoli* pv. *syngonii* (one ST), *X. euvesicatoria* ‘Philodendron’ (12 STs) and *X. citri* pv. *aracearum* (two STs), by a total of at least 35, 70 and 102 single nucleotide polymorphisms (on all genes assayed), respectively.

Among strains of *X. phaseoli* pv. *dieffenbachiae*, one to three STs were detected for a same geographic origin (Table 1).

2.2. Primer and probe design

Two sets of primers and Taqman® MGB-probes were designed, using Primer Express® software v3.0 (Thermo Fisher Scientific, Villebon-sur-Yvette, France). The first one targeted a portion of a gene encoding a putative ABC transporter-type protein (Wzt), a component of the o-antigen lipopolysaccharide (LPS) cluster, present in all *X. phaseoli* pv. *dieffenbachiae* strains pathogenic to anthurium (Robene-Soustrade et al., 2006). Sequences from *X. phaseoli* pv. *dieffenbachiae* strain LMG 695,⁴ *X. phaseoli* pv. *dieffenbachiae* strain JV589⁵ (isolated from Reunion Island), *X. phaseoli* pv. *syngonii* pathotype strain LMG 9055⁶ (isolated in the USA), and from *X. phaseoli* pv. *syngonii* strain JW188⁷ (isolated from Reunion Island) were aligned using the Clustal-W sub-alignment tool included in MEGA 4 (Tamura et al., 2007) and checked for point mutations. Primers and probe targeted two polymorphic sites, in order to exclude the *X. phaseoli* pv. *syngonii* strains (Fig. S3).

² MH194783 to MH194829 and MK243494 to MK243528 (*atpD*), MH194830 to MH194876 and MK243599 to MK243633 (*dnaK*), MH194877 to MH194923 and MK243529 to MK243563 (*efp*), MH194924 to MH194970 and MK243564 to MK243598 (*gyrB*).

³ Sequence Type: unique sequence derived from the concatenated gene dataset.

⁴ Genbank accession DQ096647

⁵ Genbank accession MH119762

⁶ Genbank accession LSLD01000001: region 2242339..2243921

⁷ Genbank accession MH119761

Table 1
Number of strains of *X. phaseoli* pv. *dieffenbachiae* and Sequence Types for each geographic origin.

Geographic origin	Number of strains	Sequence type
Australia	4	4
Brazil	7	4
Guadeloupe	9	1, 2, 3
Italy	2	2
Jamaica	1	2
Martinique	3	1, 2
New Caledonia	5	1, 4
Poland	2	2
Puerto Rico	2	1,2
Reunion Island	6	2
Tahiti	4	2
USA (Florida)	2	1
USA (Hawaii)	2	1
Venezuela	1	2

More detailed information on strains is provided in Table S1.

A second set of primers and Taqman® probe were designed for an internal amplification process control. This internal control is an endogenous DNA sequence present in the plant sample, the *Anthurium andreaeanum* chalcone synthase gene (*CHS*), encoding for an enzyme involved in the flavonoid and anthocyanin biosynthesis pathway⁸. The primers and probe sequences (Thermo Fisher Scientific, Villebon-sur-Yvette, France) are listed in Table 2. The secondary structure of the nucleic acid targets was analyzed with mfold software (Zuker, 2003).

2.3. Duplex real-time PCR assay conditions

Primers and Taqman MGB-probe concentrations were optimized for both systems using a modified Taguchi method (Cobb and Clarkson, 1994) (data not shown). The optimized mixture (15 µl) for the duplex assay consisted of 900 nM of the primers Xad-ABC-F and Xad-ABC-R, 600 nM of the primers Anth-CHS-F and Anth-CHS-R, 125 nM of the 6-FAM-labeled Taqman-MGB probe P-Xad-ABC, 50 nM of the 5'VIC-labeled Taqman-MGB probe P-Anth-CHS, 1 × Taqman Universal PCR master mix (Thermo Fisher Scientific) and 2 µl aliquot of the DNA template. The qPCRs were performed on the ABI PRISM 7000 SDS (Thermo Fisher Scientific, Villebon-sur-Yvette, France) in 96-well optical plates and covers. The thermal cycling conditions were composed of a first step at 50 °C for 2 min, followed by a pre-denaturation step at 95 °C for 10 min and 40 cycles of denaturation at 95 °C for 15 s and annealing/extension at 65 °C for 1 min.

Positive controls (tenfold dilutions of bacterial suspensions in plant matrix) and negative controls (non-template controls (NTC): plant matrix and mix without DNA) were included in each assay. Preliminary tests showed that the high annealing temperature allowed a trade-off between the efficiency of the amplification and the specificity against non-target strains, such as *X. phaseoli* pv. *syngonii* (data not shown). The fluorescence data were collected at the end of the annealing/extension steps. The threshold cycle values (Ct) were calculated by the 7000 SDS software with thresholds fixed at 0.05. An undetermined result (NA) was automatically attributed when no Ct value was obtained.

Real-time PCR assays were also run on a StepOnePlus real-time PCR system (Thermo Fisher Scientific). Optimization steps were conducted by testing different concentrations of the bacterial and plant probes (125:50; 125:100; 250:100, measured in nM) and by testing different temperature ramp rates (20%–40%–60%–100% of the maximal ramp rate).

2.4. N-PCR conditions

The N-PCR assay was performed using the first-round primer pair PXadU/ PXadL and the nested primer pair NXadU/ NXadL (Table 2) as described previously (Robene-Soustrade et al., 2006), the only difference was the use of Taq polymerase GoTaq® Flexi (Promega, Charbonnières, France).

2.5. Calibration curves and efficiency

One g of healthy anthurium leaves (*Florida* cultivar) was ground with a Homex 6 grinder (BIOREBA, Reinach, Switzerland) in 20 ml of 10 mM Tris buffer (pH 7.2) and artificially spiked with tenfold dilutions of bacterial suspensions of four target strains (LMG 695, NCPPB 3573, LB96 and JW127) to obtain population sizes ranging from about 10² to 10⁷ CFU/ml. Extraction of total DNA was performed using the DNeasy Plant Mini Kit (Qiagen, Courtaboeuf, France) following the manufacturer's instructions. This experiment was repeated five times to obtain six replicates per strain and per level of contamination. Each sample was analyzed in triplicate for the qPCR assays and in duplicate for the N-PCR assay. Ct values obtained for the six dilution series were compiled for each strain, resulting in a total of 18 replicates for each concentration level. Standard curves were generated for each strain by plotting Cts against the logarithm of starting DNA concentrations. The reaction efficiency *E* was calculated according to the slope of the standard curves as follows: $E = 10^{\left(-\frac{1}{\text{slope}}\right)} - 1$. Standard curves and reaction efficiency analyses were performed using base R functions (3.4.3; R Development Core Team, 2017).

2.6. Analytical specificity

2.6.1. In silico specificity

The 63 bp targeted DNA region of LMG 695, including the primers and probes, was blasted (BLASTn) against the NCBI nucleotide collection (nr/nt) and the NCBI collection of draft genomes belonging to the *Xanthomonas* group (taxid:338, *n* = 659) (https://blast.ncbi.nlm.nih.gov/Blast.cgi?PAGE_TYPE=BlastSearch&BLAST_SPEC=MicrobialGenomes,database=Allgenomes,draftgenomes).

2.6.2. Analytical specificity

Analytical specificity was evaluated following the guidelines in the EPPO PM 7/98 standard and using two criteria: the inclusivity, i.e. the ability of the qPCR system to detect all strains of the target organism; and the exclusivity, i.e. the capacity to generate negative responses from non-target strains (Anonymous, 2014). Inclusivity and exclusivity were analyzed on bacterial suspensions of 50 target and 92 non-target strains, respectively (Tables S1 and S2). The set of non-target strains included: *X. citri* pv. *aracearum* and *X. euvesicatoria* “Philodendron” strains pathogenic to some aroid genera but not anthurium (group A), strains belonging to different *Xanthomonas* pathovars or species not associated with Araceae (B), saprophytic bacteria isolated from anthurium (C) and strains pathogenic to anthurium belonging to other genera (D). The bacterial suspensions were prepared from 24 h-old cultures on YPGA at 28 °C. Suspensions of target strains were adjusted to about 10⁴ CFU/ml to achieve a level 10 times greater than the detection threshold of the real-time qPCR assay (10³ CFU/ml), estimated in preliminary works. Similarly, suspensions of non-target strains were adjusted to about 10⁷ CFU/ml. Bacterial population sizes were checked by plating the suspensions on YPGA plates with a Spiral system device (Interscience, Saint-Nom-La-Bretèche, France) (Jalenques, 1988). Suspensions were boiled for 2 min, placed on ice and 2 µl aliquot was used as the template in the qPCR and PCR-based assays. Two criteria must be fulfilled to consider a sample positive: the fluorescence amplification plot must display a typical sigmoidal shape and both duplicates must test positive (Ct ≤ 36.1, see below).

⁸ Available on GenBank database (DQ421809)

Table 2
Primers and probes used in this study.

Primers/probes	Sequence 5' > 3'	Amplicon size	Target
qPCR			
P-Xad-ABC MGB (6-Fam™)	TCGTTGACCAACATCG	63 bp	putative ABC transporter hydrophilic component gene
Xad-ABC-F	AAGTCAGGCGAGGCCAGTATC		
Xad-ABC-R	AGGCCGGGAAGGATCGT		
P-Anth-CHS MGB (Vic™)	CTACTTCCGAATCACC	61 bp	Chalcone synthase gene
Anth-CHS-F	GACCAGAGCACCTACCCAGACT		
Anth-CHS-R	GCTCAACCTGGTGCTCACTGT		
N-PCR			
First round			
PXadU ^a	AGGGCTCCCATGCCGGAAT	1570 bp	putative ABC transporter hydrophilic component gene
PXadL ^a	ACGCAATGCGCAGGGGAAAT		
Nested			
NXadU ^a	AGCGCGGTACATTGTTGTTCCGT	785 bp	putative ABC transporter hydrophilic component gene
NXadL ^a	GCGGATCCTGACTGAGCAAAG		

^a Primer described in Robene-Soustrade et al., 2006.

2.7. Analytical sensitivity – Cut-off value determination

Calculations were performed using R (3.4.3; R Development Core Team, 2017). The limit of detection (LOD) was evaluated on qPCR data obtained with anthurium samples artificially spiked with different bacterial concentrations (see above). Positive samples consisted of spiked samples with different bacterial concentrations (from about 10² to 10⁷ CFU/ml) ($n = 432$) and negative samples consisted of NTC ($n = 95$).

LOD is defined as the lowest amount of analyte, which can be detected with more than a stated percentage of confidence, but not necessarily quantified as an exact value (Kralik and Ricchi, 2017). LOD_{95%} is commonly used. It is the lowest concentration that leads to at least 95% of the sample replicates being positive (Broeders et al., 2014; Burns and Valvidia, 2008).

The cut-off Ct value, i.e. the PCR cycle number above which signals are no longer interpreted as positive, was evaluated by performing an ROC analysis (receiver operating characteristic curve) (Grosdidier et al., 2017; Nutz et al., 2011). The ROC curve is a plot of the sensitivity (SE) against 1-specificity (SP), where $SP = \frac{TN}{TN+FP}$, $SE = \frac{TP}{TP+FN}$, TP is the number of true positives, FN is the number of false negatives, TN is the number of true negatives and FP is the number of false positives. Sensitivity and specificity values were calculated for each cycle of qPCR run and plotted on the graph. The Youden index J is defined as: $J = SE + SP - 1$ (Youden, 1950). The cut-off value corresponded to the point on the curve with the highest value of the Youden index, i.e. with 1-SP and SE values the closest to 0 and 1, respectively. Samples with Ct values higher than the Ct cut-off were considered negative. The probability of detection (POD) = $\frac{x}{N}$, x being the number of positive samples and N the total number of samples tested, was calculated by taking into account the estimated Ct cut-off value. For the LOD_{95%} estimation, POD was plotted against the logarithm of the bacterial concentrations associated with the serial dilution. Different nonlinear functions (probit, logit, log-log, cloglog, cauchit) were adjusted using general least squares to find the best fitting curve for the data with the nlme R package (Pinheiro J, Bates D, DebRoy S, Sarkar D and R Core Team (2018). *nlme: Linear and Nonlinear Mixed Effects Models*. R package version 3.1–137, <https://CRAN.R-project.org/package=nlme>). The function with the lowest Akaike information criterion (AIC) was selected.

2.8. Repeatability

Repeatability is the level of agreement between replicates of a sample tested under the same conditions (EPPO standard PM 7/76 (2) protocol, (Anonymous, 2010)). Repeatability was estimated from quantitative and qualitative data (binary response).

For quantitative repeatability, intra-assay coefficients of variation ($Cv = \frac{\sigma}{\mu}$) based on Ct mean values, were computed with all PCR triplicates for concentrations ranging from about 10³ CFU/ml to 10⁷ CFU/ml (120 Cv values). Inter-assay Cv values were calculated from the Ct values (PCR triplicate means) obtained for the six runs independently performed for each strain, for concentrations ranging from about 10³ CFU/ml to 10⁷ CFU/ml (20 Cv values). For qualitative data, we calculated the accordance (DA). DA is the probability of finding the same result (i.e. both negative or both positive) from two identical test portions analyzed in the same laboratory under repeatability conditions (i.e. one operator using the same apparatus and same reagents within the shortest feasible time interval) (Van der Voet and Van Raamsdonk, 2004). $DA = \left(\frac{pr}{t}\right)^2 + \left(\frac{nr}{t}\right)^2$, where pr and nr are the number of positive and negative responses, respectively, and t is the total number of responses.

2.9. Assessment of the internal control on anthurium cultivars

The Ct values obtained for the internal plant control *CHS* (Vic fluorescence) amplified from anthurium samples spiked with different bacterial loads (§ Calibration curves and efficiency) were compared by an analysis of variance (ANOVA) after Box-Cox power transformation using the MASS package (Venables and Ripley, 2002), followed by a multiple pairwise comparisons using the Tukey's test.

The amplification of the internal control was also assessed on 11 healthy commercial *Anthurium andraeanum* cultivars: *Calore*, *Casino*, *Fire*, *Florida*, *Nunzia*, *Pistache*, *Presence*, *Simba*, *Spice*, *Tropical* and *Tropical Night*. Leaf tissues (0.5 g) were ground in 10 ml of 10 mM Tris buffer (pH 7.2), centrifuged and DNA was extracted as described above. Duplex-qPCR was performed in duplicate on the different extracts.

2.10. Detection from naturally infected diseased plants

Healthy ($n = 24$) or symptomatic ($n = 35$) anthurium plants were collected from different locations in Reunion Island. The leaves were surface sterilized, by briefly wiping them with 70% (vol/vol) ethanol. Leaf lesions were ground in 20 ml/g of 10 mM Tris buffer (pH 7.2) and total DNA was extracted as described above. Fifty microliters of macerates were plated in duplicate on both YPGA and NCTM4 media in order to check the presence of *X. phaseoli* pv. *dieffenbachiae*. Doubtful bacterial colonies were tested with the *X. phaseoli* pv. *dieffenbachiae*-specific N-PCR assay. N-PCR and qPCR assays were performed on the different samples. For qPCR, internal standards, composed of total DNA extracted from ten-fold bacterial suspensions of LMG 695 (10² to 10⁷ CFU/ml) added to *A. andraeanum* cv. Florida leaf homogenates, were included in each assay.

2.11. Detection from asymptomatic, latently infected plants

In preliminary tests, anthurium plants of the cultivar Previa were found weakly susceptible to *Xanthomonas phaseoli* pv. *dieffenbachiae*, with delayed and less severe symptoms compared to a susceptible cultivar (data not shown).

Eighteen month-old plants of *Anthurium andreaeanum* cultivar Previa were split into three blocks (nine plants per block). The plants were spray-inoculated in a greenhouse, as previously described, using suspensions (about 10^7 CFU/ml) of strain JV589 (Reunion) in 10 mM Tris buffer (pH 7.2) (Robene-Soustrade et al., 2006). A control set of nine plants received only Tris buffer. The temperature in the greenhouse during the experiments ranged from 21 °C to 36 °C, the light intensity ranged from 1.74 to 11.50 lx and the relative humidity ranged from 50% to 95%. This experiment was performed twice. A visual assessment of the disease was performed for 57 days after inoculation (dai). At 15 and 56 dai, three leaves were randomly collected from each block. The leaves were surface sterilized, by briefly wiping them with 70% (vol/vol) ethanol, and 1.5 g tissues were collected from the periphery of the leaves and ground with a Homex 6 grinder in 30 ml of 10 mM Tris buffer (pH 7.2). Fifty microliters of macerates were plated in duplicate on NCTM4 medium with a Spiral device in order to enumerate culturable *X. phaseoli* pv. *dieffenbachiae* cells.

Total DNA was extracted from macerates using the DNeasy Plant Mini Kit (Qiagen, Courtaboeuf, France), according to the manufacturer's instructions, and tested with the real-time duplex quantitative PCR assay. Standard DNA dilution series were included in each assay, as described above.

3. Results

3.1. Dynamic range of *X. phaseoli* pv. *dieffenbachiae*-specific qPCR assay

The dynamic range of the duplex quantitative real-time PCR was assayed with six independent 10-fold dilution series in the plant matrix for each of the strains LMG 695, NCPPB 3573, LB96 and JW127. Considering all strains, 48 negative results (undetermined results) out of 72 and 2 out of 72 were recorded for the concentrations of 10^2 CFU/ml and 10^3 CFU/ml, respectively. A linear relationship was observed between Ct values and the logarithm of bacterial concentration down to 1×10^3 CFU/ml for all four strains, with PCR efficiency ranging from 92.1 to 102.4% and $0.94 < R^2 < 0.97$ (Fig. 1).

3.2. Cut-off determination and analytical sensitivity

ROC analysis was performed by plotting SE against 1-SP (Fig. S4). The ROC curve was used to determine the optimal cut-off point, by maximizing the Youden index. The cut-off was determined at 36.1 (Fig. 2).

This cycle cut-off value was used to transform the quantitative data in reliable qualitative results (positive or negative result). Ct values > 36.1 were considered as negative responses. One hundred percent of positive responses were obtained for samples with bacterial concentrations ranging from about 10^4 CFU/ml to 10^7 CFU/ml. At a concentration of 10^3 CFU/ml, 97.2% samples were tested positive (Ct values of 36.7 and 36.3 for two samples of JW127 strain). At 10^2 CFU/ml, only 33.3% of positive responses were obtained, linked to the fact that statistically the target was not systematically present in samples at this low concentration (Poisson distribution). Fig. 3 plots the percentage of positive samples giving a Ct value equal to or < 36.1 , versus the log of the bacterial concentrations associated with the six serial dilutions. The best fitting model to the data points was a probit model. This allowed for interpolation, which gave $LOD_{95\%} = 894$ bacteria/ml (CI 95% 407.0–1965.2). In our process, this corresponded to a theoretical number of 18 bacteria per reaction.

When running the N-PCR on the same spiked samples, 100% of the

samples were tested positive for bacterial concentrations ranging from about 10^4 CFU/ml to 10^7 CFU/ml. At a concentration of 10^3 CFU/ml, 97.9% of the samples were tested positive (1 out of 12 replicates tested was negative for the strain NCPPB 3573). At a concentration of 10^2 CFU/ml, 47.9% of the samples tested positive. The best fitting model to the data points was also a probit model and the estimated $LOD_{95\%}$ was 1224 bacteria/ml (CI 95% 618.1–2425.5), corresponding to 25 bacteria per reaction (Fig. S5).

3.3. Repeatability

Quantitative repeatability was calculated from Ct values obtained across the method's dynamic range (bacterial concentrations ranging from about 10^3 CFU/ml to 10^7 CFU/ml). Intra coefficients of variation (Cvs) calculated from all qPCR triplicates ranged from 0.09 to 6.50 with a median of 1.58. The inter Cvs computed for the four strains from the six independent series ranged from 0.76 to 7.07, with a median at 2.35. When considering the qualitative responses (positive or negative), an accordance value of 99.6% was obtained across the method's whole dynamic range.

3.4. Analytical specificity

3.4.1. In silico analyses

When blasting the 63 bp target DNA of LMG 695, including the primers and probes, against the NCBI nucleotide collection, a perfect identity was obtained with partial gene sequences encoding for a putative ABC transporter component from six strains of *X. phaseoli* pv. *dieffenbachiae* isolated from anthurium in India (XAD01, XAD02, XZD03, XAD04, XAD1 and XAD2) and with a DNA fragment from the complete genome sequence of strain LMG 695 (CP014347.1). Blasts of the target DNA against the NCBI collection of draft *Xanthomonas* genomes resulted in 100% identity with the two draft genomes of *X. phaseoli* pv. *dieffenbachiae* strains LMG 695 (JPYB01000192.1) and LMG 25940 (JPYI02000075.1). DNA regions showing 97% identity over 100% of sequence length were identified from two draft genomes of the *X. phaseoli* pv. *syngonii* strain LMG 9055 (LSLD01000001.1 and JPUO02000167.1). Similarly, DNA regions showing 94% identity over 98% of the sequence were detected from the draft genome sequence of *X. oryzae* pv. *leersiae* strain NCPPB 4346 (LHUK01000429.1) and *X. oryzae* pv. *oryzae* strain X8-1A (AFHL01000039.1). Nevertheless, four mutations were found between the two primer sequences designed from LMG 695 strain and the DNA templates of strains NCPPB 4346 and strain X8-1A, with two in the 3' part of the primers. This is likely to prevent the production of amplicons from these *X. oryzae* strains.

3.4.2. Experimental data

All target strains tested positive with the real-time quantitative PCR assay (100% inclusivity, 95% confidence interval (calculated with the Wilson score and continuity correction): 91.1–100%) with Ct values ranging from 28.4 to 30.1, a mean of 29.1 and a standard deviation of 0.4 for suspensions adjusted to 10^4 CFU/ml (Table S1). All non-target strains, except *X. euvesicatoria* pv. *allii* CFBP 6380 (Ct of 31.97), displayed negative signals (exclusivity of 98.9%, CI 95%: 93.2–99.9%) (suspensions adjusted to 10^7 CFU/ml) (Table S2). All other *X. euvesicatoria* pv. *allii* strains ($n = 10$) were tested negative. Interestingly, no amplification was detected for *X. phaseoli* pv. *syngonii* ($n = 10$). Two point mutations between the primers/probe system and the DNA template of *X. phaseoli* pv. *syngonii* strains, one at the 3' forward primer extremity and one in the middle of the probe, prevented the amplification of *X. phaseoli* pv. *syngonii* DNA.

The N-PCR assay also displayed the maximal inclusivity value when tested on the different target strains. However, the exclusivity value was lower (88.0%, CI 95%:79.2–93.6%) because the N-PCR assay did not distinguish between *dieffenbachiae* and *syngonii* pathovars.

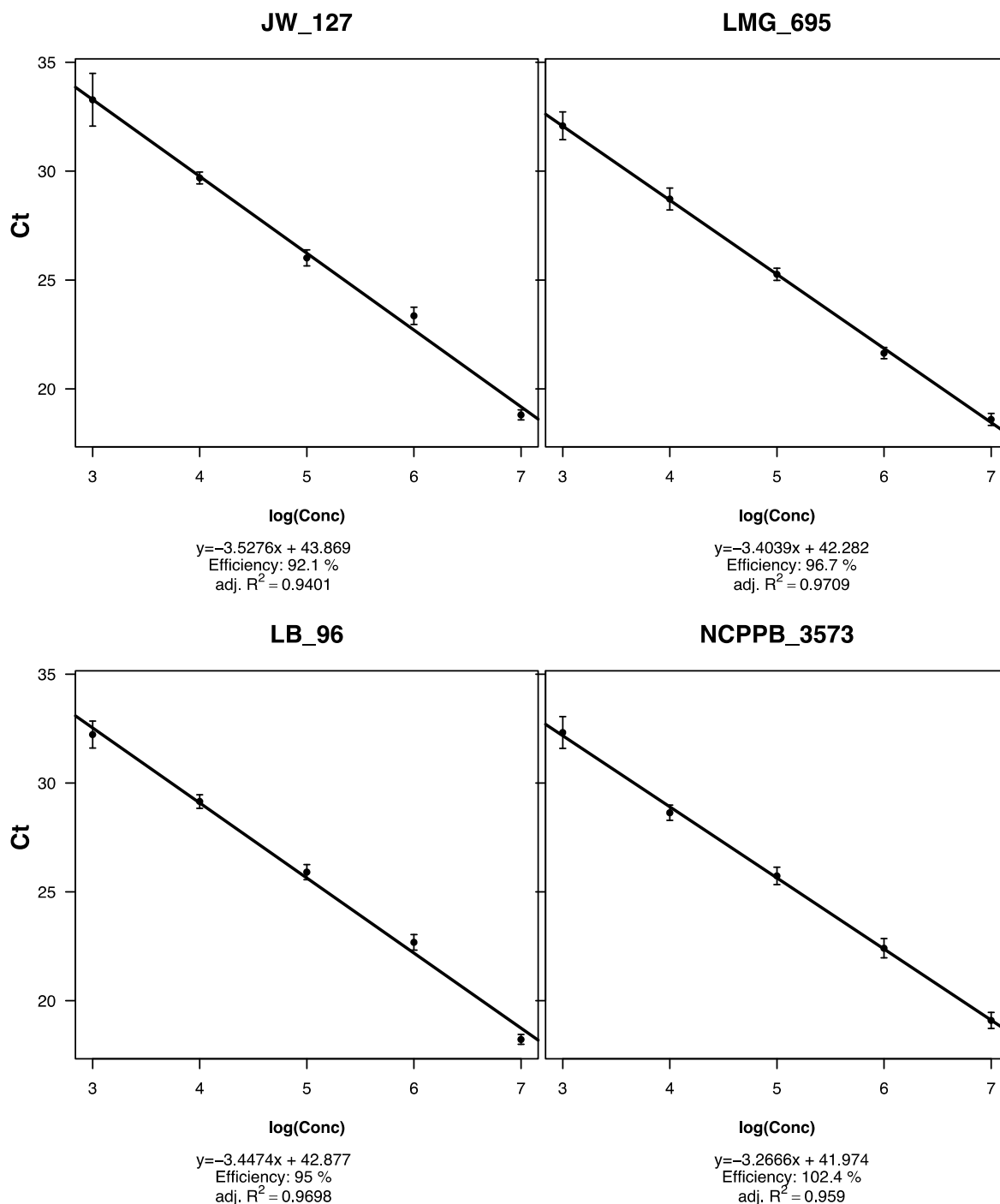


Fig. 1. Standard curves obtained from the dilution series of different *Xanthomonas phaseoli* pv. *dieffenbachiae* strains. Real-time quantitative PCR was run on genomic DNA extracted from anthurium leaves spiked with serially 10-fold diluted bacterial suspensions (10^7 to 10^2 CFU/ml) of four strains. Standard curves were constructed using linear regression analysis of the threshold cycle (Ct) values of the 10-fold dilution series over the \log_{10} of the initial target concentrations (compilation of all series and runs, corresponding to 18 replicates for each strain and at each concentration level). The linear regression equation and the adjusted R^2 are mentioned for each standard curve.

3.5. Internal control

The Ct values corresponding to the amplification of the internal plant control *CHS* (Vic fluorescence) were analyzed for the anthurium samples artificially spiked with different bacterial concentrations. All the responses with $Ct < 40$ and showing a typical fluorescence amplification curve were considered. A plant signal was detected in all plant samples without bacteria ($n = 72$) with a Ct mean value of 32.5 ± 3.9 . In the presence of bacteria the plant signal decreased as

the bacterial concentration in the assay increased: the mean Ct values for the internal plant control were 33.20 (sd = 1.14), 32.70 (sd = 1.31), 33.32 (sd = 1.59), 34.51 (sd = 1.93), 36.29 (sd = 2.13) and 37.94 (sd = 1.29) for the bacterial concentrations of 10^2 , 10^3 , 10^4 , 10^5 , 10^6 and 10^7 CFU/ml, respectively.

This competition only occurred for bacterial concentrations $\geq 10^5$ bacteria/ml. Indeed, an Anova analysis showed no significant difference between the plant Ct obtained for the three lowest bacterial concentrations (10^2 , 10^3 and 10^4 CFU/ml), whereas the Ct obtained for the

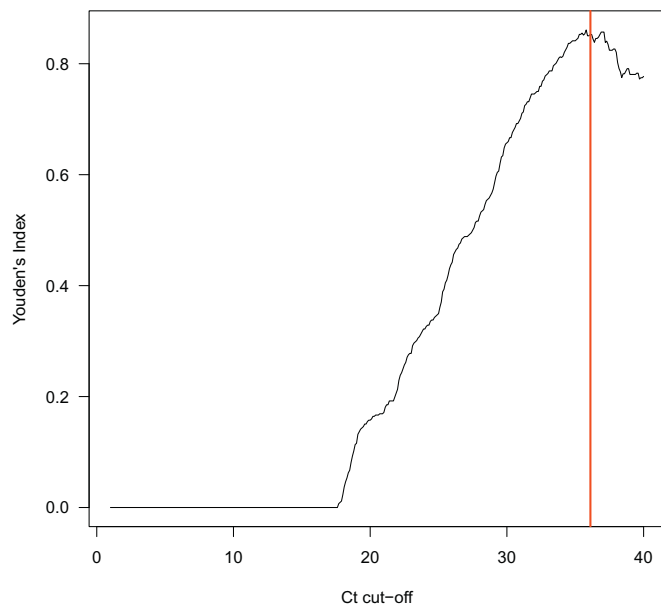


Fig. 2. Determination of the Ct cut-off according to the Youden index J . The optimal cut-off point is the PCR cycle with the highest value of the Youden index, which represents a trade-off between sensitivity and specificity. The Ct cut-off was estimated to 36.1.

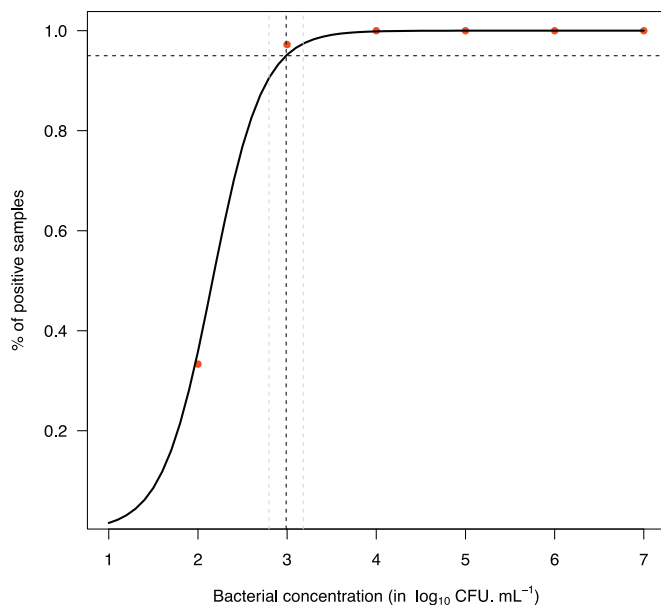


Fig. 3. Determination of the limit of detection ($LOD_{95\%}$) of the real-time qPCR assay. The x-axis represents the log of the bacterial concentrations and the y-axis represents the probability of detection (POD) of replicate samples, giving a Ct value of < 36.1 (cut-off). Each red point on the graph corresponded to 72 analyzed data. The smooth fitting line represents the model that best fits the data points, based on a least squares approach using a probit model. The dark dotted vertical line indicates the bacterial concentration corresponding to $LOD_{95\%}$ (894 CFU/ml) and the two clear dotted lines correspond to the 95% confidence interval. (For interpretation of the references to colour in this figure legend, the reader is referred to the web version of this article.)

other concentrations (10^5 , 10^6 and 10^7 CFU/ml) were all significantly different from the three others (Tuckey's p values ranged from 0.02287 to < 0.001). This pattern can be explained by a competition between the two probe/primer systems for target amplification.

In addition, the duplex-PCR was tested on a panel of healthy anthurium cultivars ($n = 11$) to verify the ability to amplify the

endogenous control in different cultivars. A plant signal was registered for all the anthurium cultivars tested, with Ct values varying from 26.67 to 32.32 and a median at 29.24.

3.6. Detection of *X. phaseoli* pv. *dieffenbachiae* from naturally infected plants

A series of 34 symptomatic anthurium samples, originating from different locations in Reunion Island, were analyzed using both qPCR, N-PCR and isolation on both YPGA and NCTM4 media (Table S3). The qPCR assay successfully detected the presence of *X. phaseoli* pv. *dieffenbachiae* in 34 out of 35 symptomatic samples (Cts < 36.1 for each replicate), whereas the N-PCR assay was slightly less efficient with 31 positive samples out of 35 samples. The isolation method was the least effective, only 21 out of 35 samples tested positive. The sample 9 M was the only one from which *X. phaseoli* pv. *dieffenbachiae* was isolated (only one colony, identity confirmed by PCR using PXadU and PXadL primers), whereas both real-time PCR and N-PCR assays yielded a negative result. The 24 healthy anthurium plants were tested negative by both molecular methods and isolation. It is important to note that 10 other symptomatic plants collected by field inspectors as ABB tested negative with the three methods. This suggests that they displayed confusing symptoms, not caused by *X. phaseoli* pv. *dieffenbachiae*. It confirms that visual diagnostics are unreliable. SP value and corresponding CI 95% was 100% (86.2–100) for the three methods. SE value was 97.1 (85.5–99.5) for qPCR, 88.6% (74.1–95.5) for N-PCR and 60% (43.6–74.5) for the isolation method.

3.7. Detection of *X. phaseoli* pv. *dieffenbachiae* from asymptomatic anthurium plants

Typical ABB symptoms were first recorded at 21 to 44 dai, depending on the block. Therefore, all samples analyzed at 15 dai were asymptomatic. Real-time quantitative detection was successfully achieved with 9 samples showing bacterial concentrations higher than the LOD value (and at least one leaf sample among three for the blocks 1 to 5) (Fig. 4). Colonies of *X. phaseoli* pv. *dieffenbachiae* were also recovered from NCTM4 plates, indicating that at least a fraction of the target population was actually viable. This was further confirmed by the subsequent development of ABB from these plants. Overall, population sizes derived from NCTM4 plating experiments were lower than those obtained using the real-time PCR assay. In four samples, the pathogen was solely detected by PCR.

3.8. Transferability of the qPCR assay

The qPCR assay could be adapted to the StepOnePlus Real-Time PCR system by doubling probe concentrations both for plant and bacterial systems, with a ramp rate maintained at 100% to obtain a correct plant signal (Efficiency = 93.7, $R^2 > 0.99$). A reliable plant signal could be obtained for healthy samples and for samples with bacterial concentrations ranging from about 10^2 to 10^5 CFU/ml. Undetermined results were obtained from higher bacterial concentrations.

4. Discussion

This paper describes the development of a real-time duplex PCR for the detection and quantification of *X. phaseoli* pv. *dieffenbachiae*, which represents the greatest sanitary threat to anthurium worldwide.

The diagnostic of ABB was historically based on isolation of the pathogen followed by phenotypic characterization (biochemical and pathogenicity tests). In addition, an N-PCR developed previously (Robene-Soustrade et al., 2006) displayed a high level of specificity and a level of sensitivity suitable for the detection of bacteria from symptomless plants (Chabirand et al., 2014). The major drawback of N-PCR assays is the risk of carry-over contamination. Real-time quantitative

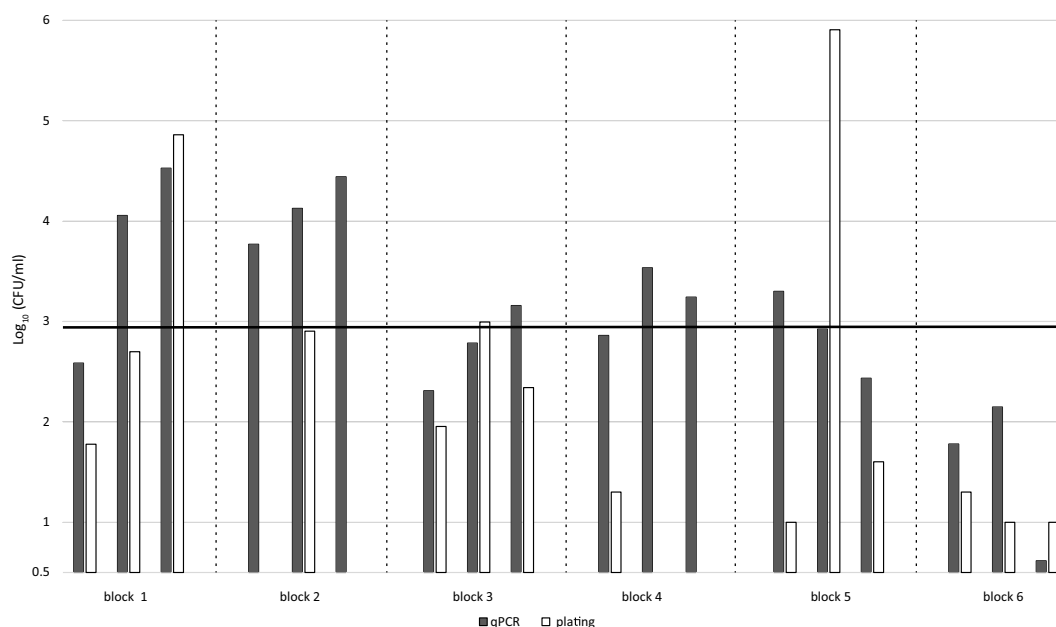


Fig. 4. Detection of *Xanthomonas phaseoli* pv. *dieffenbachiae* from asymptomatic anthurium plants. Plants of *Anthurium andreaeanum* cultivar Previa were spray-inoculated with strain JV589 (Reunion) under greenhouse conditions. At 15 dai, three asymptomatic leaves per block were analyzed using real-time quantitative PCR assay and plating on semi-selective medium NCTM4. This experiment was repeated over time: Experiment 1 - blocks 1, 2 and 3; Experiment 2 - blocks 4, 5 and 6. No bar appears when *Xanthomonas phaseoli* pv. *dieffenbachiae* was not detected. Horizontal bar: $\text{LOD}_{95\%} = 2.95$ (concentration of 894 bacteria/ml).

PCR technology is increasingly used in the field of diagnostic microbiology because it has many major advantages over classical PCR: shorter turnaround time, the system is more contained and it includes quantitative analysis. Compared to a real-time PCR, N-PCR is also more labor-intensive (two PCR steps, gel electrophoresis required).

The Taqman probe/primer system developed here targets the *wzt* gene, component of a LPS cluster. Alignment with *X. phaseoli* pv. *syngonii* sequences revealed some point mutations used to design a specific set of primers and probe. The high specificity of the system was confirmed with a panel of strains representing the diversity of *X. phaseoli* pv. *dieffenbachiae*, *X. phaseoli* pv. *syngonii* and other taxa isolated from anthurium or other aroid genera (Table S2). No reliable amplification was observed for non-target bacteria, except for a single *X. euvesicatoria* pv. *allii* strain (CFBP 6380) pathogenic to several *Allium* species (Roumagnac et al., 2004). The N-PCR assay, as well as an indirect ELISA using a *X. phaseoli* pv. *dieffenbachiae*-specific monoclonal antibody, previously tested positive for this strain Robene-Soustrade et al. (2006). The LPS locus in plant pathogenic bacteria, as in animal pathogens, is under intense diversifying selection and several studies conducted for different *Xanthomonas* lineages provided evidence for horizontal transfer and rearrangements in a gene region of the LPS cluster including the *wzt* gene (Patil et al., 2007; Wasukira et al., 2014; Zhang et al., 2015). We hypothesize that CFBP 6380 may host a xenologous *wzt* gene, yielding a positive reaction both by DNA amplification and serology-based detection methods. In any event, pathogenicity assays showed that strain CFBP 6380 was not pathogenic to anthurium. Thus, this cross-reaction should not interfere in the diagnosis of *X. phaseoli* pv. *dieffenbachiae* because most xanthomonads have a highly restricted host range (Leyns et al., 1984) and the presence of this strain on anthurium plants is highly improbable. If necessary, a RFLP-PCR is available to distinguish this *X. euvesicatoria* pv. *allii* strain from the *X. phaseoli* pv. *dieffenbachiae* strains (Robene-Soustrade et al., 2006). Consistent with *in silico* predictions, qPCR did not produce a positive signal for the closely related *X. phaseoli* pv. *syngonii* strains, which share syngonium as a host with *X. phaseoli* pv. *dieffenbachiae*. Exclusivity was therefore improved, as compared to N-PCR.

In addition to the set of primers and probe for the detection of *X. phaseoli* pv. *dieffenbachiae*, we developed an internal control of qPCR,

based on the amplification of the *CHS* in *Anthurium andreaeanum*, the most common commercial host species. This internal control amplification attests that the different processes such as total DNA extraction and amplification have worked (process control). Experimentally, we verified that the plant signal was correctly amplified on a set of 11 different commercial *Anthurium andreaeanum* cultivars. Our target sequence is contiguous to partial coding sequences of chalcone synthase available on NCBI for 99 different *Anthurium* species and shows a very high identity level with the *A. andreaeanum* sequence (> 97–100%) (Carlsen and Croat, 2013). It is probable that most of the *Anthurium* species would be amplified by our qPCR system.

An inhibition of the plant signal was shown when high bacterial concentrations were present in the extracts, indicating probable competition for target amplification between the two primer/probe systems. Nevertheless, this plant control is especially useful for confirming that the process has worked correctly in the absence of a positive signal for the target bacterium. We demonstrated successful amplification of the plant target for bacterial concentrations ranging from 0 to 10^8 CFU/ml.

Weak real-time PCR signals corresponding to high Ct values were sometimes registered for negative controls due to low cross-over contaminations and/or probe fluorescence background emission (Burns and Valvidia, 2008; Caraguel et al., 2011). This phenomenon is very common when running real-time PCR. Several methods are available to determine a reliable Ct cut-off value, i.e. the PCR cycle number above which any response is considered as a false positive (Grosdidier et al., 2017; Nutz et al., 2011; Robene et al., 2015). We used the statistical approach based on ROC analysis, where both false positive and false negative responses were considered to implement a reliable Ct cut-off value. The estimated cycle threshold of 36.1 was applied to determine the level of sensitivity of the qPCR assay. $\text{LOD}_{95\%}$ was estimated at 894 CFU/ml (CI 95% 407.0–1965.2), which corresponded to 18 bacteria per reaction. Theoretically, $\text{LOD}_{95\%}$ can be as low as 3 targets when only the Poisson distribution contributes to replicate variation (Stahlberg and Kubista, 2014). For real samples, LOD can be influenced by different parameters, e.g. the plant matrix, DNA extraction and qPCR steps, and it can be significantly higher.

The sensitivity of the N-PCR was slightly lower, with a detection

threshold around 10^3 CFU/ml ($\text{LOD}_{95\%} = 1224$ CFU/ml, CI 95% 618.1–2425.5). This sensitivity level is consistent with previous studies (Chabirand et al., 2014; Robène-Soustrade et al., 2006).

One advantage of a real-time quantitative assay is the high level of repeatability. The values for the intra- and inter-repeatability coefficient of variations calculated for the Ct values over the method's whole dynamic range were < 8%, which is perfectly acceptable compared to the commonly used threshold of 25% (Broeders et al., 2014). High values of accordance between replicates (99.5%) were also obtained when considering qualitative responses.

Real-time quantitative detection of *X. phaseoli* pv. *dieffenbachiae* was evidenced from both naturally symptomatic infected plants and asymptomatic latently infected plants. In this last case, the cultivar used was found partially resistant to ABB. Here, we demonstrated the importance of using the real-time PCR assay for detecting latent infections and, thereby, reducing the risk of introducing the pathogen during material exchanges. The isolation method on NCTM4 semi-selective medium was found to be less effective for detecting *X. phaseoli* pv. *dieffenbachiae*. The rapid development of non-target bacteria on agar plates probably prevented some of the target bacteria from growing. This limitation of the use of semi-selective media for the recovery of bacterial strains from environmental samples is well known (Kawanishi et al., 2011). The N-PCR assay failed to detect a few infected samples compared to the qPCR assay. This could be correlated with this molecular tool's slightly lower sensitivity level.

The qPCR assay was successfully run using different real-time PCR equipment after a few adjustments. It would be interesting in the future to test the portability on other real-time PCR instruments via inter-laboratory assays, as already performed for the N-PCR assay (Chabirand et al., 2014).

To conclude, we developed a qPCR assay that displayed greater specificity, sensitivity and reliability compared to the previously available N-PCR assay (Robène-Soustrade et al., 2006). This real-time PCR assay could be helpful for indexing propagative plant material, monitoring regional outbreaks and monitoring imported plant material in areas free of ABB.

Supplementary data to this article can be found online at <https://doi.org/10.1016/j.mimet.2019.03.003>.

Funding

This work was supported by grants from the Conseil Régional de La Réunion, the European Union Agricultural Fund for Rural Development (EAFRD) and the European Regional Development Fund (ERDF) and by the French Ministry of Overseas Territories, the French Ministry of Agriculture and Food and the CIRAD.

Acknowledgments

The authors gratefully acknowledge Jessica Barthet, Flora Nice, Marion Perret (CIRAD), Aurélie Moreau (ANSES), Jacques Fillatre (ARMEFLHOR) and Janice Minatchy (FDGDON) and the Plant Protection Platform (3P, IBISA) for their assistance.

References

Alvarez, A.M., Toves, P.J., Vowell, T.S., 2006. Bacterial blight of anthuriums: Hawaii's experience with a global disease. *APSNet Feat.* <https://doi.org/10.1094/APSnetFeature-2006-0206>.

Anonymous, 2009. *Xanthomonas axonopodis* pv. *dieffenbachiae*. *EPPD Bull.* 39, 393–402.

Anonymous, 2010. EPPD standards-use of EPPD diagnostic protocols. *PM7/76(2)*. *EPPD Bull.* 40, 350–352.

Anonymous, 2014. *Diagnostics - PM 7/98 (2)* specific requirements for laboratories preparing accreditation for a plant pest diagnostic activity. *EPPD Bull.* 44, 117–147.

Berthier, Y., Verdier, V., Guesdon, J.L., Chevrier, D., Denis, J.B., Decoux, G., Lemattre, M., 1993. Characterization of *Xanthomonas campestris* pathovars by rRNA gene restriction patterns. *Appl. Environ. Microbiol.* 59, 851–859.

Broeders, S., Huber, I., Grohmann, L., Berben, G., Taverniers, I., Mazzara, M., Roosens, N.,

Morisset, D., 2014. Guidelines for validation of qualitative real-time PCR methods. *Trends Food Sci. Tech.* 37, 115–126.

Bui Thi Ngoc, L., Vernière, C., Jouen, E., Ah-You, N., Lefeuvre, P., Chiroleu, F., Gagnevin, L., Pruvost, O., 2010. Amplified fragment length polymorphism and multilocus sequence analysis-based genotypic relatedness among pathogenic variants of *Xanthomonas citri* pv. *citri* and *Xanthomonas campestris* pv. *bilvae*. *Int. J. Syst. Evol. Microbiol.* 60, 515–525.

Burns, M., Valvidia, H., 2008. Modelling the limit of detection in real-time quantitative PCR. *Eur. Food Res. Technol.* 226, 1513–1524.

Caraguel, C.G., Stryhn, H., Gagne, N., Dohoo, I.R., Hammell, K.L., 2011. Selection of a cutoff value for real-time polymerase chain reaction results to fit a diagnostic purpose: analytical and epidemiologic approaches. *J. Vet. Diagn. Investig.* 23, 2–15.

Carlsen, M.M., Croat, T.B., 2013. A molecular phylogeny of the species-rich neotropical genus *Anthurium* (Araceae) based on combined chloroplast and nuclear DNA. *Syst. Bot.* 38, 576–588.

Chabirand, A., Jouen, E., Pruvost, O., Chiroleu, F., Hostachy, B., Bergsma-Vlami, M., Bianchi, G., Cozzolino, L., Elphinstone, J., Holvea, M., Manole, F., Martini, P., Matoušková, H., Minatchy, J., Op de Beeck, G., Poliakov, F., Sigillo, L., Siverio, F., Van Vaerenbergh, J., Laurentie, M., Robène-Soustrade, I., 2014. Comparative and collaborative studies for the validation of a nested PCR for the detection of *Xanthomonas axonopodis* pv. *dieffenbachiae* from anthurium samples. *Plant Pathol.* 63, 20–30.

Chase, A.R., Stall, R.E., Hodge, N.C., Jones, J.B., 1992. Characterization of *Xanthomonas campestris* strains from aroids using physiological, pathological, and fatty acid analysis. *Phytopathology* 82, 754–759.

Cobb, B.D., Clarkson, J.M., 1994. A simple procedure for optimising the polymerase chain reaction (PCR) using modified Taguchi methods. *Nucleic Acids Res.* 22, 3801–3805.

Constantin, E.C., Cleenwerck, L., Maes, M., Baeyen, S., Van Malderghem, C., De Vos, P., Cottyn, B., 2016. Genetic characterisation of strains named as *Xanthomonas axonopodis* pv. *dieffenbachiae* leads to a taxonomic revision of the *X. axonopodis* species complex. *Plant Pathol.* 65, 792–806.

Constantin, E.C., Haegeman, A., Van Vaerenbergh, J., Baeyen, S., Van Malderghem, C., Maes, M., Cottyn, B., 2017. Pathogenicity and virulence gene content of *Xanthomonas* strains infecting Araceae, formerly known as *Xanthomonas axonopodis* pv. *dieffenbachiae*. *Plant Pathol.* 66, 1539–1554.

Dickey, R.S., Zumoff, C.H., 1987. Bacterial leaf blight of *Syngonium* caused by a pathovar of *Xanthomonas campestris*. *Phytopathology* 77, 1257–1262.

Garces, F.F., Gutierrez, A., Hoy, J.W., 2014. Detection and quantification of *Xanthomonas albilineans* by qPCR and potential characterization of sugarcane resistance to leaf scald. *Plant Dis.* 98, 121–126.

Grosdidier, M., Aguayo, J., Marçais, B., Ios, R., 2017. Detection of plant pathogens using real-time PCR: how reliable are late Ct values? *Plant Pathol.* 66, 359–367.

Guindon, S., Gascuel, O., 2003. A simple, fast, and accurate algorithm to estimate large phylogenies by maximum likelihood. *Syst. Biol.* 52, 696–704.

Hamza, A.A., Robène-Soustrade, I., Jouen, E., Lefeuvre, P., Chiroleu, F., Fischer-Le Saux, M., Gagnevin, L., Pruvost, O., 2012. Multilocus sequence analysis- and amplified fragment length polymorphism-based characterization of xanthomonads associated with bacterial spot of tomato and pepper and their relatedness to *Xanthomonas* species. *Syst. Appl. Microbiol.* 35, 183–190.

Ios, R., Fourrier, C., Iancu, G., Gordon, T.R., 2009. Sensitive detection of *Fusarium circinatum* in pine seed by combining an enrichment procedure with a real-time polymerase chain reaction using dual-labeled probe chemistry. *Phytopathology.* 99, 582–590.

Jalenques, F., 1988. Dénombrement rapide de colonies microbiennes par le "Système Spiral". *Inf. Tech. Biol.* 1, 13–16.

Joubert, J.J., Truter, S.J., 1972. A variety of *Xanthomonas campestris* pathogenic to *Zantedeschia aethiopia*. *Neth. J. Plant Path.* 78, 212–217.

Kawanishi, T., Shiraishi, T., Okano, Y., Sugawara, K., Hashimoto, M., Maejima, K., Komatsu, K., Kakizawa, S., Yamaji, Y., Hamamoto, H., Oshima, K., Namba, S., 2011. New detection systems of bacteria using highly selective media designed by SMART: selective medium-design algorithm restricted by two constraints. *PLoS One* 6, e16512.

Kralik, P., Ricchi, M., 2017. A basic guide to real time PCR in microbial diagnostics: definitions, parameters, and everything. *Front. Microbiol.* 8, 108.

Laurent, P., Chabirand, A., Jouen, E., Robène-Soustrade, I., Gagnevin, L., Hostachy, B., Pruvost, O., 2009. A new semi-selective medium for the isolation of *Xanthomonas axonopodis* pv. *dieffenbachiae*, the etiological agent of anthurium bacterial blight. *Letters Appl. Microbiol.* 49, 210–216.

Leyns, F., De Cleene, M., Swings, J.G., De Ley, J., 1984. The host range of the genus *Xanthomonas*. *Bot. Rev.* 50, 308–356.

Li, W.B., Hartung, J.S., Levy, L., 2006. Quantitative real-time PCR for detection and identification of *Candidatus* Liberibacter species associated with citrus Huanglongbing. *J. Microbiol. Methods* 66, 104–115.

Lipp, R.L., Alvarez, A.M., Benedict, A.A., Berestecky, J., 1992. Use of monoclonal antibodies and pathogenicity tests to characterize strains of *Xanthomonas campestris* pv. *dieffenbachiae* from aroids. *Phytopathology* 82, 677–682.

Muska, A., Peck, E., Palmer, S., 2007. Standards and controls: concepts for preparation and use in real-time PCR application. In: Mackay, I.M. (Ed.), *Real-time PCR in Microbiology: From Diagnosis to Characterization*. Caister Academic Press, Norfolk, UK, pp. 101–131.

Niu, J.H., Gao, Y.R., Yin, J.M., Leng, Q.Y., Yang, G.S., Wang, C., Ren, Y., 2015. Development and evaluation of a loop-mediated isothermal amplification assay for rapid detection of bacterial blight pathogen (*Xanthomonas axonopodis* pv. *dieffenbachiae*) in anthurium. *Eur. J. Plant Pathol.* 142, 801–813.

Nutz, S., Doll, K., Karlovsky, P., 2011. Determination of the LOQ in real-time PCR by receiver operating characteristic curve analysis: application to qPCR assays for

- Fusarium verticillioides* and *F. proliferatum*. Anal. Bioanal. Chem. 401, 717–726.
- Palacio-Bielsa, A., Cubero, J., Cambra, M.A., Collados, R., Berruete, I.M., Lopez, M.M., 2011. Development of an efficient real-time quantitative PCR protocol for detection of *Xanthomonas arboricola* pv. *pruni* in *Prunus* species. Appl. Environ. Microbiol. 77, 89–97.
- Parkinson, N., Cowie, C., Heeney, J., Stead, D., 2009. Phylogenetic structure of *Xanthomonas* determined by comparison of *gyrB* sequences. Int. J. Syst. Evol. Microbiol. 59, 264–274.
- Patil, P.B., Bogdanove, A.J., Sonti, R.V., 2007. The role of horizontal transfer in the evolution of a highly variable lipopolysaccharide biosynthesis locus in xanthomonads that infect rice, citrus and crucifers. BMC Evol. Biol. 6.
- Robbs, C.F., 1955. Algumas bacterias fitopatogenicas do distrito federal. Agronomia 14, 147–164.
- Robene, I., Perret, M., Jouen, E., Escalon, A., Maillot, M.V., Chabirand, A., Moreau, A., Laurent, A., Chiroleu, F., Pruvost, O., 2015. Development and validation of a real-time quantitative PCR assay to detect *Xanthomonas axonopodis* pv. *allii* from onion seed. J. Microbiol. Meth. 114, 78–86.
- Robene-Soustrade, I., Laurent, P., Gagnevin, L., Jouen, E., Pruvost, O., 2006. Specific detection of *Xanthomonas axonopodis* pv. *dieffenbachiae* in anthurium (*Anthurium andreaeanum*) tissues by nested PCR. Appl. Environ. Microbiol. 72, 1072–1078.
- Roumagnac, P., Gagnevin, L., Gardan, L., Sutra, L., Manceau, C., Dickstein, E.R., Jones, J.B., Rott, P., Pruvost, O., 2004. Polyphasic characterization of xanthomonads isolated from onion, garlic and Welsh onion (*Allium* spp.) and their relatedness to different *Xanthomonas* species. Int. J. Syst. Evol. Microbiol. 54, 15–24.
- Schoulties, C.L., Civerolo, E.L., Miller, J.W., Stall, R.E., Krass, C.J., Poe, S.R., Ducharme, E.P., 1987. Citrus canker in Florida. Plant Dis. 71, 388–395.
- Stahlberg, A., Kubista, M., 2014. The workflow of single-cell expression profiling using quantitative real-time PCR. Expert. Rev. Mol. Diagn. 14, 323–331.
- Tamura, K., Dudley, J., Nei, M., Kumar, S., 2007. MEGA4: molecular evolutionary genetics analysis (MEGA) software version 4.0. Mol. Biol. Evol. 24, 1596–1599.
- Van der Voet, H., Van Raamsdonk, L.W.D., 2004. Estimation of accordance and concordance in inter-laboratory trials of analytical methods with qualitative results. Int. J. Food Microbiol. 95, 231–234.
- Venables, W.N., Ripley, B.D., 2002. Modern Applied Statistics With S. Springer, New York, NY, USA.
- Wasukira, A., Coulter, M., Al-Sowayeh, N., Thwaites, R., Paszkiewicz, K., Kubiriba, J., Smith, J., Grant, M., Studholme, D.J., 2014. Genome sequencing of *Xanthomonas vasicola* pathovar vasculorum reveals variation in plasmids and genes encoding lipopolysaccharide synthesis, type-IV pilus and type-III secretion effectors. Pathogens 3, 211–237.
- Youden, W.J., 1950. Index for rating diagnostic tests. Cancer. 3, 32–35.
- Zhang, Y., Jalan, N., Zhou, X., Goss, E., Jones, J.B., Setubal, J.C., Deng, X., Wang, N., 2015. Positive selection is the main driving force for evolution of citrus canker-causing *Xanthomonas*. ISME J. 9, 2128–2138.
- Zuker, M., 2003. Mfold web server for nucleic acid folding and hybridization prediction. Nucleic Acids Res. 31, 3406–3415.